Detection of ECG Characteristic Points Using Wavelet Transforms

Cuiwei Li, Chongxun Zheng, and Changfeng Tai

Abstract—**An algorithm based on wavelet transforms (WT's) has been developed for detecting ECG characteristic points. With the multiscale feature of WT's, the QRS complex can be distinguished from high P or T waves, noise, baseline drift, and artifacts. The relation between the characteristic points of ECG signal and those of modulus maximum pairs of its WT's is illustrated. By using this method, the detection rate of QRS complexes is above 99.8% for the MIT/BIH database and the P and T waves can also be detected, even with serious baseline drift and noise.**

I. Introduction

THE AUTOMATIC detection of ECG waves is important to cardiac disease diagnosis. A good performance of an automatic ECG analyzing system depends heavily upon the accurate and reliable detection of the QRS complex, as well as the T and P waves.

The detection of the QRS complex is the most important task in automatic ECG signal analysis. Once the QRS complex has been identified, a more detailed examination of ECG signal, including the heart rate, the ST segment, etc., can be performed. The algorithms for QRS detectors can generally be divided into three categories: 1) nonsyntactic, 2) syntactic, and 3) hybrid. The algorithms based on a syntactic approach are time-consuming, due to the need for grammar inference for each class of patterns [15]. So, most of the applicable QRS detectors are nonsyntactic [1], [7], [9], [10]. Generally, these detectors first filter the ECG signal with a bandpass filter (or a matched filter) to suppress the P and T waves and noise. Then, the signal will be passed through a nonlinear transformation, for example, derivative and square, etc., to enhance the QRS complexes. Finally, decision rules are used to determine whether QRS complexes are present in the signal. These techniques mainly suffer from two problems: 1) the signal frequency band of the QRS complex is different for different subjects and even for different beats of the same subject; and 2) the frequency bands of the noise and QRS complex overlap. Although a matched filter [1] can improve the signal-to-noise ratio, its effect is limited by the variability of QRS waveforms for different beats of the same subject.

The detection of the P wave is difficult because this wave is small and sometimes is embedded in noise. One method to detect the P wave has been described by Jenkins [4], in which an esophageal electrode is used to get high-amplitude P waves. This method can not be widely applied due to the uncomfortable sensation caused by the esophageal electrode and lead wire. Other algorithms for P wave detection, including the syntactic method [5] and the hidden Markov method [6], are complex and time-consuming. Gritzali proposed a simple method to detect P and T waves by "length transformation" [7], but it is not robust to noise.

Wavelet transform is a very promising technique for time-frequency analysis. By decomposing signals into elementary building blocks that are well localized both in time and frequency, the WT can characterize the local regularity of signals [3]. This feature can be used to distinguish ECG waves from serious noise, artifacts and baseline drift. In this paper, an algorithm based on the WT for detecting QRS complex, P and T waves is proposed. A dyadic wavelet transform is used for extracting ECG characteristic points. The local maxima of the WT modulus at different scales can be used to locate the sharp variation points of ECG signals. The algorithm first detects the QRS complex, then the T wave, and finally the P wave.

II. Theory

A. Wavelet Transform

The WT of a signal $f(x)$ is defined as

$$W_s f(x) = f(x) * \Psi_s(x) = \frac{1}{s}\int_{-\infty}^{+\infty} f(t)\Psi\left(\frac{x-t}{s}\right)dt \quad (1)$$

where s is scale factor. $\Psi_s(x) = \frac{1}{s}\Psi(\frac{x}{s})$ is the dilation of a basic wavelet $\psi(x)$ by the scale factor s. Let $s = 2^j$ ($j \in Z$, Z is the integral set), then the WT is called dyadic WT [3]. The dyadic WT of a digital signal $f(n)$ can be calculated with Mallat algorithm [11] as follows:

$$S_{2^j} f(n) = \sum_{k\in Z} h_k S_{2^{j-1}} f(n - 2^{j-1}k) \quad (2)$$

$$W_{2^j} f(n) = \sum_{k\in Z} g_k S_{2^{j-1}} f(n - 2^{j-1}k) \quad (3)$$

where S_{2^j} is a smoothing operator and $S_{2^0} f(n) = d_n$. d_n is the digital signal to be analyzed [13], which is the ECG signal used in this paper. $W_{2^j} f(n)$ is the WT of digital signal $f(n)$. $\{h_k \mid k \in Z\}$ and $\{g_k \mid k \in Z\}$ are coefficients of a lowpass filter $H(\omega)$ and a highpass filter $G(\omega)$, respectively [13]; that means

$$H(\omega) = \sum_{k\in Z} h_k e^{-ik\omega}, \quad G(\omega) = \sum_{k\in Z} g_k e^{-ik\omega}.$$

Manuscript received December 27, 1993; revised September 8, 1994. This work was supported by the Foundation of the State Education Commission of China under grant No. 9269813.

The authors are with the Biomedical Engineering Institute of Xi'an Jiaotong University, Xi'an, Shaanxi, 710049, P. R. China.

IEEE Log Number 9406725.

The wavelet we used is a quadratic spline wavelet with compact support and one vanishing moment. It is a first derivative of a smooth function [13]. The Fourier transform of $\psi(x)$ is

$$\hat{\Psi}(\omega) = i\omega\left(\frac{\sin\frac{\omega}{4}}{\frac{\omega}{4}}\right)^4.$$

The symbol $\wedge$ represents the discrete Fourier transform. The filters $H(\omega)$ and $G(\omega)$ are

$$H(\omega) = e^{i\omega/2}\left(\cos\frac{\omega}{2}\right)^3 \tag{4}$$

$$G(\omega) = 4ie^{i\omega/2}\left(\sin\frac{\omega}{2}\right). \tag{5}$$

B. Equivalent Filter of WT

The discrete Fourier transform of WT is [13]

$$\begin{aligned}\hat{W}_{2^j} f(\omega) &= \hat{f}(\omega)\hat{\Psi}(2^j\omega) \\ &= \begin{cases} G(\omega)\hat{f}(\omega)\hat{\phi}(\omega) & j=1 \\ G(2\omega)H(\omega)\hat{f}(\omega)\hat{\phi}(\omega) & j=2 \\ G(2^{j-1}\omega)H(2^{j-2}\omega)\cdots H(\omega)\hat{f}(\omega)\hat{\phi}(\omega) & j>2 \end{cases}\end{aligned} \tag{6}$$

where ϕ is a smooth function, and $\hat{f}(\omega)\hat{\phi}(\omega)$ is the discrete Fourier transform of the ECG signal d_n $(n \in Z)$ [13]. From (6), the WT of $f(n)$ at scale 2^j is equal to a filtered signal of d_n that passed through a digital bandpass filter (or high pass filter for scale 2^1). Let $Q^j(\omega)$ be the transform function of the equivalent filter. Then, we have

$$Q^j(\omega) = \begin{cases} G(\omega) & j=1 \\ G(2\omega)H(\omega) & j=2 \\ G(2^{j-1}\omega)H(2^{j-2}\omega)\cdots H(\omega) & j>2. \end{cases} \tag{7}$$

From (4), (5), and (7), we can deduce (see Appendix)

$$Q^j(\omega) = \frac{2}{8^{j-1}} \sum_{k=1-2^{j-1}}^{2^j+2^{j-1}-2} q_k^j e^{ik\omega} \tag{8}$$

$$q^j_{1-2^{j-1}+k} = -q^j_{2^j+2^{j-1}-2-k} \neq 0,$$
$$k \in [1-2^{j-1}, 2^j+2^{j-1}-2]$$

where $Q^j(\omega)$ is an FIR digital filter with generalized linear phase [2]. The filter is antisymmetric and the time delay of its central point is $\frac{2^j-1}{2}$ (the delay is considered as $2^{j-1}-1$ points in the algorithm). According to the form of the quadratic spline wavelet [11], we know that every uniphase wave, like the (a) or (b) waves in Fig. 1, corresponds to a positive maximum-negative minimum pair of $W_{2^j}f(n)$ at different scales. The wave rising edge corresponds to a negative minimum, and the dropping edge corresponds to a positive maximum at different scales. The moduli of these maxima or minima corresponding to the same edge are named as the modulus maximum line. If the uniphase wave is symmetric to its peak, as shown in Fig. 1(a), then its peak corresponds to the zero-crossing point of the positive maximum-negative minimum pair with a delay of exactly $2^{j-1}-1$ points. If the uniphase wave is not symmetric to its peak, as shown in Fig. 1(b), then the peak corresponds to the zero-crossing point of the positive maximum-negative minimum pair with a delay of about $2^{j-1}-1$ points. The larger the scale, the bigger is the error between the delay and $2^{j-1}-1$. At small scale 2^1, the error is zero. At large scale, the error is still tolerant. For example, in Fig. 1(b), the slope of rising edge is three times larger than that of the dropping edge, but the error is only two points at scale 2^4.

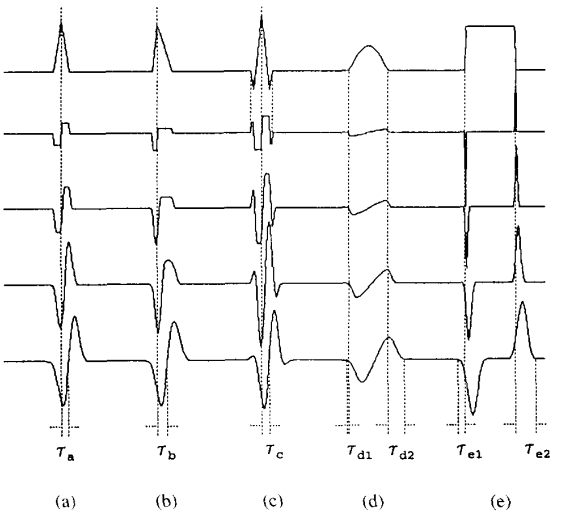

Fig. 1. The relation between the characteristic points of simulation waves and those of their WT's at different scales. The uniphase wave (a) is symmetric and $T_a = 2^{4-1}-1 = 7$ points. The uniphase wave (b) is not symmetric and $T_b - T_a = 2$ points. Complex (c) is symmetric and $T_c = T_a = 7$ points. In waves (d) and (e), $T_{d1} < T_{e1}, T_{d2} < T_{e2}, T_{e1} = 2^{4-1}-1 = 7$ points and $T_{e2} = 2^4 + 2^{4-1} - 2 = 22$ points.

From (8), we can see that the beginning point of q_k^j is at $1-2^{j-1}$, and the ending point of q_k^j is at $2^j + 2^{j-1} - 2$. So, the onset of a uniphase wave corresponds to the onset of a positive maximum-negative minimum pair with a delay of $1-2^{j-1}$ points, and the offset corresponds to an offset with a delay of $2^j + 2^{j-1} - 2$ points, as shown in Fig. 1(e).

Corresponding to 250/s ECG sampling rate, the amplitude-frequency responses of the equivalent digital filters $Q^j(\omega)$ $(j = 1, 2, \ldots, 5)$ are illustrated in Fig. 2, and their 3-dB bandwidths are listed in Table I.

C. Relation Between the Signal Singularity and its WTS

Signal singularities often carry the most important information. It is important to find the location of singularity and characterize the singular degree in signal processing. The singular degree is often described with the Lipschitz exponent [11]. On the pioneer work of Grossman [12], Mallat founded the relation between the WT's and singularities of signals [11]. If wavelet $\psi(x)$ is the first derivative of a smooth function, then

1) When scale s is small enough, the maxima of $|W_s f(x)|$ indicate the locations of sharp variation signal points.

2) The function $f(x)$ is Lipschitz α $(0 < \alpha < 1)$ over $[a, b]$, if and only if there exists a constant A such that for all $x \in [a, b]$,

$$|W_{2^j} f(x)| \leq A(2^j)^\alpha. \tag{9}$$

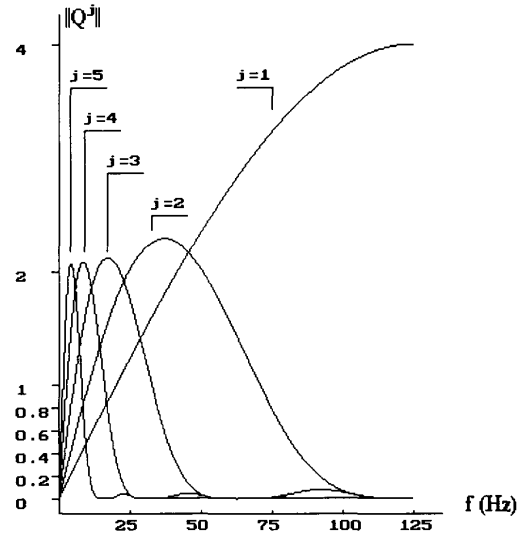

Fig. 2. The amplitude-frequency responses of equivalent filter $Q^j(\omega)$ at different scales corresponding to 250/s sampling rate. $f = 125\omega/\pi$.

TABLE I
THE 3-dB BANDWIDTHS OF EQUIVALENT FILTER $Q^j(\omega)$ AT DIFFERENT SCALES

scale	3 db bandwidth (Hz)
$s=2^1$	62.5 ~ 125.0
$s=2^2$	18 ~ 58.5
$s=2^3$	8 ~ 27
$s=2^4$	4 ~ 13.5
$s=2^5$	2 ~ 6.5

III. DETECTION METHODS

A. R Peak Detection

We analyzed 600 data points of an ECG signal each time. The WT's of ECG signals are calculated with (2) and (3), then the decision rules are applied for detection. A more detailed description of the detection procedure is given as follows:

1) Selection of Characteristic Scales: From Fig. 2, it can be seen that the $W_{2^j}f(n)$ at small scales reflects the high frequency components of the signal and, at large scales, reflects the low frequency components of the signal. According to the power spectra of the ECG signal, noise and artifact [8], and the 3-dB bandwidths of $Q^j(\omega)$ shown in Table I, it is clear that most energies of the QRS complex are at the scales of 2^3 and 2^4, and the energy at scale 2^3 is the largest. From scale 2^3 to smaller or larger scales, the energy of the QRS complex decreases gradually. According to our experiments, for QRS complex with more high frequency components, the energy at scale 2^2 is larger than that at scale 2^3, and for the QRS complex with more low frequency components, the energy at scale 2^4 is larger than that at scale 2^3. For larger scales 2^j ($j \geq 5$), the energy of the QRS complex is decreased further and, at the same time, the energies of motion artifact and noise are increased. Furthermore, the selection of more scales requires more calculations. So, we only select scales from 2^1 to 2^4. These scales are called characteristic scales in this paper.

2) Determination of Modulus Maximum Lines of R Waves: From Fig. 1(a), we can see that the wave corresponds to two modulus maximum lines with opposite signs of $W_{2^j}f(n)$. The modulus maximum lines corresponding to R waves at characteristic scales must be determined. A method to select these modulus maxima from large to small scale is as follows:

Step 1: Find all of the modulus maxima larger than a threshold ε_4 at scale 2^4 to obtain the location set of modulus maxima $\{n_k^4 \mid k = 1 \cdots N\}$;

Step 2: Find a modulus maximum larger than the threshold ε_3 on the neighborhood of n_k^4 at scale 2^3 and define its location as n_k^3. If several modulus maxima exist, then the largest one is selected. But, the modulus maximum with its location nearest n_k^4 will be selected if the largest one is not larger than 1.2 times the others. If no modulus maximum exists, then set n_k^3, n_k^2, and n_k^1 to zero. So, the location set $\{n_k^3 \mid k = 1 \cdots N\}$ can be found.

Step 3: Similar to Step 2, the locations of the modulus maxima at scales 2^2 and 2^1 are found. Then, the location sets $\{n_k^2 \mid k = 1 \cdots N\}$ and $\{n_k^1 \mid k = 1 \cdots N\}$ will be obtained.

By searching modulus maxima at characteristic scales, the location set of modulus maximum lines $\{n_k^4, n_k^3, n_k^2, n_k^1 \mid k = 1 \cdots N\}$ is obtained. By eliminating those modulus maximum lines with $n_k^1 = 0$, the location set of remaining modulus maximum lines is $\{n_k^4, n_k^3, n_k^2, n_k^1 \mid k = 1 \cdots N_1\}$.

Searching the modulus maxima from large to small scale has two reasons. First, the number of modulus maxima at large scale are much fewer than those at small scale, so searching the modulus maxima from large to small scale can save calculating time. Second, high frequency noise decays greatly at large scale so that it creates no modulus maximum or a very small one. Therefore, by using an appropriate threshold to detect modulus maxima at large scale, the faulty detections caused by high frequency noise can be reduced greatly. The modulus maxima detected at large scale may also include those induced by P and T waves, as well as the baseline drift. But their effects at small scale are slight because their high frequency energies are trifling. Using a threshold for these modulus maxima at small scale can also eliminate their effects.

3) Calculation of Singular Degree: Let $a_j(n_k) = |W_{2^j} f(n_k)|$ and suppose α is the upper bound of the Lipschitz exponent. α is called the regularity exponent [3]. From (9), we can deduce the regularity exponent [14]

$$\alpha \approx \log_2 a_{j+1}(n_k) - \log_2 a_j(n_k). \tag{10}$$

Let

$$\alpha_j = \log_2 a_{j+1}(n_k^{j+1}) - \log_2 a_j(n_k^j) \tag{11}$$

where α_j represents the decay of $|W_{2^j} f(n_k)|$ over the scales and is an approximation of the Lipschitz exponent at singularity n_k. If characteristic scales are set from 2^J to 2^{J+N}, then

α_j can be calculated from $j = J$ to $j = J + N - 1$. When the scale is large enough, $a_j(n_k)$ will decrease to zero, no matter the regularity of the signal at n_k [3]. In fact, when $j \to +\infty$, then [3]

$$a_j(n) = \mathrm{O}\left(\frac{1}{2^j}\right).$$

Hence, from (11), we can deduce $\alpha_j \leq -1$ if j is big enough. So, small scales should be selected [3], in order to avoid $\alpha_j \leq -1$. Therefore, $\alpha' = \frac{\alpha_J + \cdots \alpha_{J+N-1}}{N}$ will be a better approximation of the regularity exponent α.

At the characteristic scales from 2^1 to 2^4, we can calculate the α_1, α_2, and α_3 of a singularity point. The R wave always corresponds to $\alpha_1 > 0$, and mostly $\alpha_2 > 0$. Although some modulus maxima of R waves with higher frequency components decay fast at large scale to make $\alpha_2 \leq 0$, $\alpha_1 + \alpha_2$ is still greater than zero. For most R waves, their energies at scale 2^3 are larger than those at scale 2^4, and the decay of $|W_{2^j} f(n_k)|$ from 2^3 to 2^4 is large enough to make not only $\alpha_3 < 0$, but also $\alpha_1 + \alpha_2 + \alpha_3 \leq 0$. For high frequency noise and interference with sharp irregularities, there are also $\alpha_1 \leq 0$, $\alpha_2 \leq 0$, and $\alpha_3 \leq 0$, hence $\alpha_1 + \alpha_2 + \alpha_3 \leq 0$. So, from the value of $\alpha_1 + \alpha_2 + \alpha_3$, the R wave, high frequency noise, and interference can not be distinguished. Therefore, only α_1 and α_2 are selected and we let $\alpha' = \frac{\alpha_1 + \alpha_2}{2}$ in order to make $\alpha' > 0$ for most of the normal R waves. For distorted R waves, the increasing of the low frequency components can only make α' much larger. So, if the α' suddenly decreases greatly or even becomes negative, the corresponding singularity point must be noise or interference, which will be eliminated.

4) Elimination of Isolation and Redundant Modulus Maximum Lines: The frequency bands of motion artifact and muscle noise often overlap with that of the QRS complex. Ordinary bandpass filters can not eliminate or even decrease their effects. In the location set of modulus maximum lines, there may be those created by motion artifact and muscle noise. By eliminating isolation and redundant modulus maximum lines, we can greatly reduce the effects of motion artifact and muscle noise.

First, eliminate isolation modulus maximum lines. The R wave corresponds to a positive maximum-negative minimum pair at each characteristic scale and the interval of its two modulus maxima at scale 2^1 is shorter than its width, as shown in Fig. 1(a). Suppose n_1^1 is the location of a positive maximum (negative minimum) of $W_{2^j} f(n)$ at scale 2^1, and n_k^1 $(k = 1 \cdots N_1, k \neq 1)$ is the location of a negative minimum (positive maximum) of $W_{2^j} f(n)$ at the same scale. If the interval between n_1^1 and n_k^1 $(k \neq 1)$ is larger than an interval threshold, the maximum (minimum) at n_1^1 is considered the isolation maximum (minimum). The corresponding modulus maximum line is an isolation line and should be eliminated from the set of modulus maximum lines. The selected interval threshold should be approximately the same as the interval of the two modulus maxima created by the widest possible QRS complex in order that wide QRS complexes are not lost and artifacts and noise are mostly eliminated. In this paper, the interval threshold is empirically defined as 120 ms.

Next, eliminate redundant modulus maximum lines. Usually, the R wave corresponds to only two modulus maximum lines. But, for some dual R waves or noise in the neighborhood (120 ms) of a modulus maximum line, there are two or more modulus maximum lines, only one of which is useful; the others are redundant. The redundant modulus maximum lines are eliminated by the rules described below.

Because the main energy of the QRS complex is at scale 2^3, the modulux maxima at this scale is analyzed. For example, in the neighborhood (120 ms) of a positive maximum, there are two negative minimum. Let the two minima be Min1 and Min2, their absolute values be A_1 and A_2, respectively, and the intervals between the minima and maximum beL_1 and L_2, respectively. The rules of judging redundant modulus maximum lines are as follows:

Rule 1: If $A_1/L_1 > 1.2A_2/L_2$, Min2 is redundant.

Rule 2: If $A_2/L_2 > 1.2A_1/L_1$, Min1 is redundant.

Rule 3: Otherwise, if Min1 and Min2 are on the same side of the positive maximum, then the minimum farther from the maximum is redundant. If Min1 and Min2 are on different sides of the maximum, then the minimum following the maximum is redundant.

With these judging rules, the R wave edge with the larger slope and amplitude, or the positive R wave (corresponding to positive maximum after negative minimum in a modulus maximum pair) is selected.

A similar procedure is implemented for the case of one negative minimum and two positive maxima, and the redundant modulus maximum lines can also be eliminated.

5) Detection of the R Peak: According to the relation between signal characteristic points and those of WT depicted in Section II, R peak can be located at a zero-crossing point of a positive maximum-negative minimum pair at scale 2^1. After we eliminate the isolation and redundant lines from the location set of modulus maximum lines, $n_k^1 (k = 1, 2 \cdots N_2)$ in the remaining set is only composed of the locations of the positive maximum-negative minimum pairs at scale 2^1. Thus, the zero-crossing points of these positive maximum-negative minimum pairs are found to obtain the locations of R peaks.

In R peak detection, four thresholds $\{\epsilon_1, \epsilon_2, \epsilon_3, \epsilon_4\}$ are used for the modulus maxima detection at four different scales. These thresholds are updated by the modulus maximum of WT's of the most recently recognized QRS complex as follows:

$$\begin{aligned} &\text{If } |W_{2^j} f(n_k^j)| \geq 2A_j^m \quad \text{then } A_j^{m+1} = A_j^m; \\ &\qquad\qquad\qquad\qquad \text{else } A_j^{m+1} = 0.875A_j^m \\ &\qquad\qquad\qquad\qquad\qquad + 0.125|W_{2^j} f(n_k^j)|. \\ &\text{Let } \epsilon_j = 0.3A_j^{m+1} \qquad j = 1, 2, 3, 4 \end{aligned}$$

where $|W_{2^j} f(n_k^j)|$ is the modulus maximum of WT corresponding to the R wave. When $|W_{2^j} f(n_k^j)| \geq 2A_j^m$, the parameter A_j^{m+1} maintains its original value so that the sudden increase of the QRS amplitude would not effect the next judging.

In most cases, the algorithm correctly detects the R peak. However, some tactics based on pioneer work [10] are still used to improve the detection.

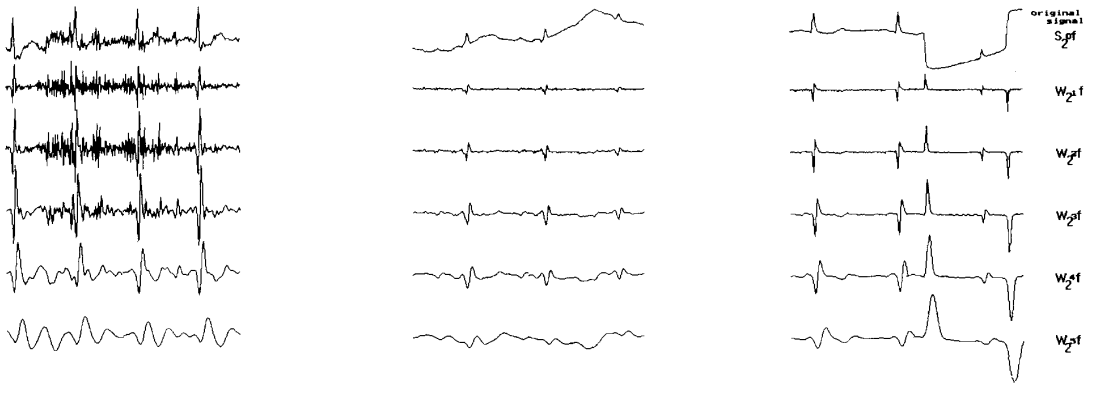

Fig. 3. ECG signals and their WT's at scale 2^1 to 2^5. The modulus maxima of WT of the QRS complexes at scale 2^3 are largest. The effects of high frequency noise are mainly at small scales, as shown in (a). The effects of baseline drift are mainly at large scales, as shown in (b). An artifact in (c) creates an isolation modulus maximum in a certain time.

Tactic 1: Blanking, where events immediately following a QRS detection are ignored for a period of 200 ms.

Tactic 2: Searching back, where previously rejected events are reevaluated when a significant time has passed without finding a QRS complex. If no QRS complex was detected within 150% of the latest average RR interval, then we detect the modulus maxima again at scale 2^3 with a threshold of 0.5 ϵ_3. If a positive maximum and negative minimum of WT are detected and the interval between them is less than 120 ms, then their zero-crossing point is detected and the reevaluated R peak can be found with a modification of 3 $(= 2^{3-1} - 1)$ points delay.

B. QRS Onset and Offset Detection

After the detection of R peaks, the onset and offset of the QRS complex are also detected. The onset of the QRS complex is defined as the beginning of the Q wave (or R wave when Q wave is not present), and the offset of the QRS complex is defined as the ending of the S wave (or R wave when the S wave is not present).

Ordinarily, the Q and S waves are high frequency and low amplitude waves and their energies are mainly at small scale. So, we detect the onsets and offsets of QRS complexes at scale 2^1. From the (c) wave in Fig. 1, we can see that the onset of QRS corresponds to the beginning of the first modulus maximum before the modulus maximum pair created by the R wave, and the offset of QRS corresponds to the ending of the first modulus maximum after that modulus maximum pair. From the modulus maximum pair of the R wave, the beginning and ending of the first modulus maxima before and after the modulus maximum pair are detected within a time window. The reason for detecting the beginning and ending points at scale 2^1, rather than at the original signal, is to avoid the effect of baseline drift.

C. T and P Wave Detection

After the detection of the QRS complex, the peaks, onsets, and offsets of T and P waves are also detected. According to the power spectra of ECG signal, noise and artifact [8] and the passbands of filter $Q^j(\omega)$ at different scales in Table I, the energies of T and P waves are mainly at scales 2^4 and 2^5. But, baseline drift is serious at scale 2^5, so scale 2^4 is selected to detect T and P waves.

The T wave creates a pair of modulus maxima with a different sign of $W_{2^j}f(n)$ at scale 2^4, within a time window after the detected R peak. Because the T wave is almost symmetric to its peak, the peak of the T wave corresponds to the zero-crossing point of the modulus maximum pair with a 7 $(2^{4-1} - 1)$ point delay. The onset and offset of the T wave correspond to the onset and offset of the modulus maxima pair with delays of -7 $(1 - 2^{4-1})$ and 22 $(2^4 + 2^{4-1} - 2)$ points, respectively. In practice, the points near the onset and offset of the modulus maximum pair are also approximately zero because the T wave is smoothed by the equivalent filter $Q^j(\omega)$ at large scale, so those actually detected are inside the interval between the onset and offset of the modulus maximum pair, as shown in Fig. 1(d). When we detect the onset and offset of the modulus maxima pair, the onset is actually modified with a delay of -2 points and the offset is 17 points. These practice delays are empirical.

The peak, onset, and offset of the P wave are detected similarly to those of the T wave within a time window before the detected R wave.

IV. Results

We used the MIT/BIH arrhythmia database to evaluate our algorithm. Only channel 1 of the two-channel ECG signal in the database was used. The WT's of some ECG signals with serious high frequency noise, baseline drift, and artifacts are shown in Fig. 3. In Table II, we list QRS detection rates for records of the MIT/BIH database. The WT algorithm produces 65 false positive (FP) beats (0.05%) and 112 false negative (FN) beats (0.1%) for a total detection failure of 177 beats (0.15%). Record 105 is more noisy than the others; Record 108 has unusually high and sharp P waves; Record 203 has a great number of QRS complexes with multiform ventricular

TABLE II
THE RESULTS OF THE QRS DETECTION ALGORITHM FOR THE MIT/BIH DATABASE

Type	Total (beats)	FP (beats)	FN (beats)	Failed detection (beats)	Failed detection (%)
100	2273	0	0	0	0
101	1865	1	0	1	0
102	2187	0	0	0	0.11
103	2084	0	0	0	0
104	2230	8	2	10	0.45
105	2572	15	13	28	1.09
106	2027	2	3	5	0.25
107	2137	0	0	0	0
108	1763	13	15	28	1.59
109	2532	0	0	0	0
111	2124	1	1	2	0.09
112	2539	2	1	3	0.12
113	1795	2	0	2	0.11
114	1879	3	0	3	0.16
115	1953	0	0	0	0
116	2412	0	1	1	0.04
117	1535	1	0	1	0.07
118	2275	1	0	1	0.04
119	1987	1	0	1	0.05
121	1863	2	1	3	0.16
122	2476	0	0	0	0
123	1518	0	0	0	0
124	1619	0	0	0	0
200	2601	0	1	1	0.04
201	1963	1	12	13	0.66
202	2136	0	1	1	0.05
203	2982	2	24	26	0.87
205	2656	0	1	1	0.04
207	1862	2	3	5	0.27
208	2956	0	4	4	0.14
209	3004	0	0	0	0
210	2647	3	3	6	0.23
212	2748	0	0	0	0
213	3251	0	0	0	0
217	2208	1	1	2	0.09
219	2154	0	0	0	0
220	2048	0	0	0	0
221	2427	0	7	7	0.29
222	2484	1	9	10	0.40
223	2605	0	2	2	0.08
228	2053	3	7	10	0.49
230	2256	0	0	0	0
231	1886	0	0	0	0
232	1780	0	0	0	0
233	3079	0	0	0	0
234	2753	0	0	0	0
TOTALS:	116137	65	112	177	0.15

arrhythmia; and Record 222 has some non-QRS waves with highly unusual morphologies. These records often create more QRS detection errors with other algorithms [9], [10], but significant improvement was achieved with our WT algorithm.

Some ECG records with artifact, serious noise, and baseline drift are illustrated in Fig. 4, in which the detected characteristic points are marked.

V. CONCLUSION AND DISCUSSION

In this paper, we present an algorithm based on WT for the detection of QRS, T, and P waves of ECG. There are several distinct features to our method.

1) With multiscale information, it is easy to characterize the ECG waves, and the QRS complex is easy to distinguish from high P and T waves, noise, baseline drift, and interference.
2) A quadratic spline wavelet with compact support is used. It has generalized linear phase so there is a determinate relation between ECG characteristic points and the modulus maxima, or the zero-crossing points, of the WT's.
3) A QRS complex corresponds to a modulus maxima pair of the WT. On the contrary, an artifact having only a rising or dropping edge in a certain time corresponds

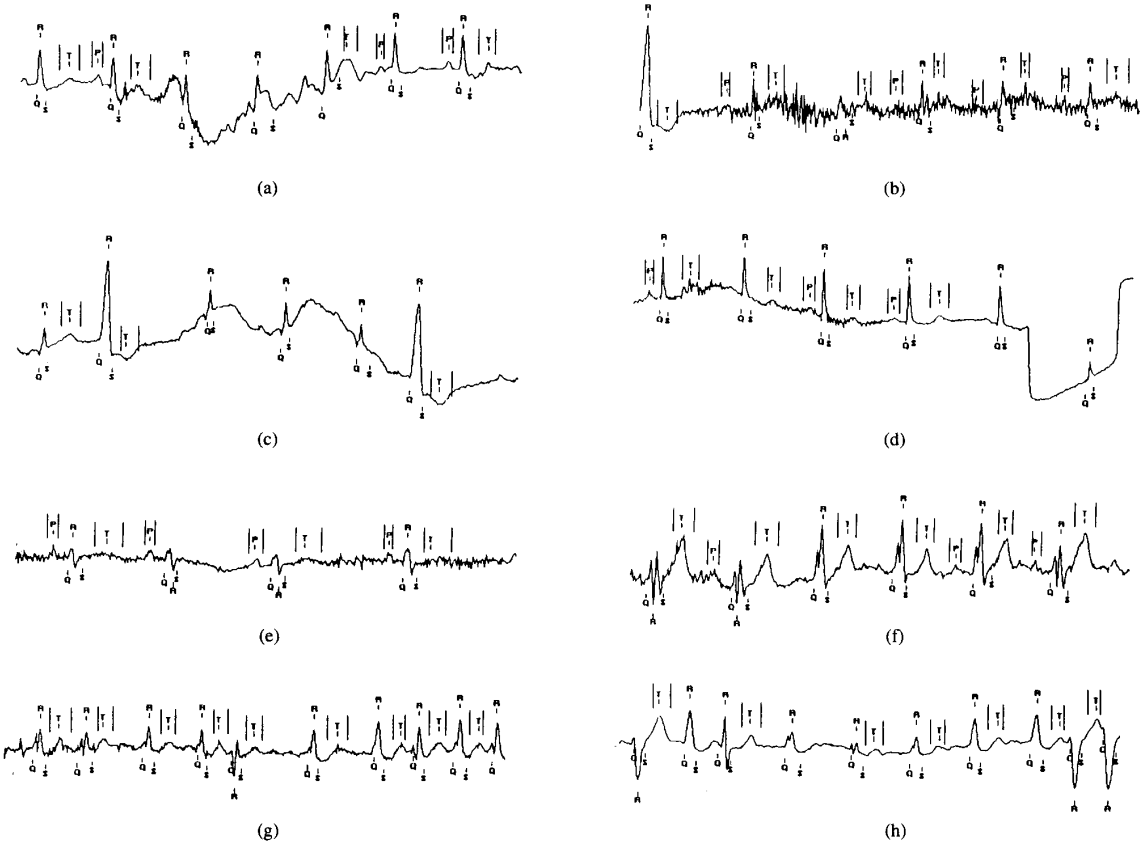

Fig. 4. The detected ECG waves. The symbol R marks the locations of R peaks, where the positive R waves are marked above and the negative ones are marked below. The symbols Q and S mark the beginning and ending locations of QRS complexes. The symbols P and T mark the peak locations and widths of P and T waves, respectively. (a) and (b) Different noise. (c) Baseline drift. (d) Artifacts. (e) High P waves. (f) High T waves. (g) and (h) Multiform ventricular arrhythmia beats.

to only one modulus maximum of the WT. So, the algorithm can greatly reduce the effect of artifact.

4) The algorithm can detect not only QRS complex, but also the T and P waves. So, other detailed characteristics, for example, ST segment and RR rate, etc., can easily be obtained.

Besides the quadratic spline wavelet, we also used higher order spline wavelets, whose Fourier transforms are as follows:

$$\hat{\Psi}(\omega) = i\omega\left(\frac{\sin\omega/4}{\omega/4}\right)^{2n+1} \qquad n = 2, 3, 4.$$

The equivalent filters of the WT's using these wavelets have bandwidths approximating those of the quadratic spline wavelet, so the results of ECG detection with these wavelets are almost the same as those with quadratic spline wavelet. But, the coefficient series of their equivalent filters is longer than that of the quadratic spline wavelet, so more time is required to calculate their WT's.

Daubechies' orthonormal wavelets [16] are also used in our experiments. But, the orthonormal wavelet does not have linear phase or generalized linear phase [2], so no determinate relation between the characteristic points of ECG and those of their WT's can be found. Therefore, these wavelets do not give detection results as good as the spline wavelets.

From the results, we know that the onsets and offsets of P and T waves may not be detected to an accuracy required for morphological diagnosis when they are influenced seriously by noise or baseline drift or their amplitudes are too small. Also, only the uniphase P and T waves are considered in this paper. This method can be considered for further development and supplemented with other techniques for the biphase P and T waves, and this will be our further research work.

The algorithm is implemented on a 486-DX33 personal computer with C Language. Processing 10 min ECG data (250/s sampling rate) requires 1 min, on average. This speed is not good enough to analyze long-time ambulatory ECG data. But, this algorithm is promising with higher speed computers or microprocessors.

The algorithm for detecting ECG characteristic points based on WT shows the potential of the WT, especially for processing time-varying biomedical signals. The power of WT lies in its multiscale information analysis which can characterize a signal very well. It is clear that the WT method will lead to a new way of biomedical signal processing.

APPENDIX
ANTISYMMETRIC CHARACTERISTIC OF THE EQUIVALENT FILTER $Q^j(\omega)$

From (4), (5), and (7), we have

$$\begin{aligned} j=1, \quad & Q^j(\omega) = 2(e^{i\omega}-1) \\ j=2, \quad & Q^j(\omega) = \frac{1}{4}(e^{4i\omega}+3e^{3i\omega}+2e^{2i\omega}-2e^{i\omega}-3-e^{-i\omega}). \end{aligned} \tag{A1}$$

From (4), we know

$$H(2^j\omega) = \frac{1}{8}(e^{2^{j+1}i\omega}+3e^{2^j i\omega}+3+e^{-2^j i\omega}) \tag{A2}$$

so $H(2^j\omega)$ $(j \in Z)$ is a symmetric filter. Let

$$P(\omega) = H(2^{j-2}\omega)\cdots H(\omega) \qquad j>2.$$

Then, from (A2), we can deduce that $P(\omega)$ is also a symmetric filter, where

$$\begin{aligned} P(\omega) &= \frac{1}{8^{j-1}} \sum_{k=1-2^{j-1}}^{2^j-2} p_k e^{ik\omega} \qquad j>2 \\ p_{1-2^{j-1}+k} &= p_{2^j-2-k} \neq 0 \quad k \in [1-2^{j-1} \quad 2^j-2]; \end{aligned} \tag{A3}$$

therefore

$$\begin{aligned} Q^j(\omega) &= G(2^{j-1})\omega P(\omega) \quad j>2 \\ &= \frac{2}{8^{j-1}}\left(\sum_{k=2^j-1}^{2^j+2^{j-1}-2} p_{k-2^{j-1}}e^{ik\omega} + \sum_{k=1}^{2^j-2} \right. \\ &\quad \left. \times(p_{k-2^{j-1}}-p_k)e^{ik\omega} - \sum_{k=1-2^{j-1}}^{0} p_k e^{ik\omega}\right). \end{aligned} \tag{A4}$$

From (A3) and (A4), we get

$$j>2, \qquad Q^j(\omega) = \sum_{k=1-2^{j-1}}^{2^j+2^{j-1}-2} q_k^j e^{ik\omega}$$

$$q_k^j = \begin{cases} p_k & k \in [1-2^{j-1}, 0] \\ p_{k-2^{j-1}} - p_k & k \in [1, 2^j-2] \\ p_{k-2^{j-1}} & k \in [2^j-1, 2^j+2^{j-1}-2] \end{cases} \tag{A5}$$

$$\begin{aligned} q^j_{1-2^{j-1}+k} &= -q^j_{2^j+2^{j-1}-2-k} \neq 0 \\ & k \in [1-2^{j-1}, 2^j+2^{j-1}-2]. \end{aligned}$$

From (A1) and (A5), we know the equivalent filter $Q^j(\omega)$ is antisymmetric whose central point is at $\frac{2^j-1}{2}$.

REFERENCES

[1] Q. Z. Xie, Y. H. Hu, and W. J. Tompkins, "Neural-network based adaptive matched filtering of QRS detection," *IEEE Trans. Biomed. Eng.*, vol. 39, pp. 317–329, 1992.

[2] C. K. Chui, *Wavelet Analysis and its Applications*. New York: Academic Press, 1992.

[3] S. Mallat and W. L. Hwang, "Singularity detection and processing with wavelets," *IEEE Trans. Inform. Theory*, vol. 38, pp. 617–643, 1992.

[4] J. M. Jenkins, D. Wu, and R. C. Arzbaecher, "Computer diagnosis of supraventricular and ventricular arrhythmias," *Circ.*, vol. 60, pp. 977–985, 1979.

[5] E. Skordalakis, "Syntactic ECG processing: A review," *Pattern Recog.*, vol. 19, pp. 305–313, 1986.

[6] D. A. Coast, R. M. Stern, G. G. Cano, and S. A. Briller, "An approach to cardiac arrhythmia analysis using hidden Markov model," *IEEE Trans. Biomed. Eng.*, vol. 37, pp. 826–835, 1990.

[7] F. Gritzali, G. Frangakis, and G. Papakonstantinou, "Detection of the P and T waves in an ECG," *Comput. Biomed. Res.*, vol. 22, pp. 83–91, 1989.

[8] N. V. Thakor, J. G. Webster, and W. J. Tompkins, "Estimation of QRS complex power spectra for design of a QRS filter," *IEEE Trans. Biomed. Eng.*, vol. BME-31, pp. 702–705, 1984.

[9] J. Pan and W. J. Tompkins, "A real-time QRS detection algorithm," *IEEE Trans. Biomed. Eng.*, vol. BME-32, pp. 230–236, 1985.

[10] P. S. Hamilton and W. J. Tompkins, "Quantitative investigation of QRS detection rules using the MIT/BIH arrhythmia database," *IEEE Trans. Biomed. Eng.*, vol. BME-33, pp. 1157–1187, 1986.

[11] S. Mallat, "Zero-crossings of a wavelet transform," *IEEE Trans. Inform. Theory*, vol. 37, pp. 1019–1033, 1991.

[12] A. Grossman, "Wavelet transform and edge detection," in *Stochastic Processes in Physics and Engineering*, M. Hazewinkel, Ed. Dodrecht: Reidel, 1986.

[13] S. Mallat, "Characterization of signals from multiscale edges," *IEEE Trans. Pattern Anal. Machine Intell.*, vol. 14, pp. 710–732, 1992.

[14] C. Z. Qiang, "A study of fault diagnosis and cutting chatter with wavelets," *Chinese J. Huazhong Univ. Sci. and Tech.*, vol. 21, pp. 88–94, 1993.

[15] E. Pietka, "Feature extraction in computerized approach to the ECG analysis," *Pattern Recog.*, vol. 24, pp. 139–146, 1991.

[16] I. Daubechies, "Orthonormal bases of compactly supported wavelets," *Commun. Pure Appl. Math.*, vol. 41, pp. 909–996, 1988.

Cuiwei Li received the M.S. degree in automatic control in 1991, and the Ph.D. degree in biomedical engineering in 1994 from Xi'an Jiaotong University, China.

She is now with the Biomedical Engineering Institute of Xi'an Jiaotong University, where she is working on biomedical signal processing.

Chongxun Zheng received the diploma in electrical engineering from Xi'an Jiaotong University, China, in 1962.

He worked in the Department of Electrical Engineering, Xi'an Jiaotong University from 1962 to 1981. He was as a Visiting Scholar in King's College of London and Brunel University, U.K., from 1981 to 1983. He joined the Department of Information and Control Engineering, Xi'an Jiaotong University from 1984 to 1990, where he was an Associate Professor, and then a Professor (since 1988). He is currently a Professor and the Director of the Research Institute of Biomedical Engineering at the same university. His research interests include biomedical signal processing and applications, cardiac electrophysiology, speech recognition, and diagnosis and reliable design of digital systems.

Changfeng Tai was born in Shaanxi, China, on May 27, 1966. He received the B.S., M.S., and Ph.D. degrees in biomedical engineering from Xi'an Jiaotong University, China, in 1986, 1989, and 1992, respectively.

He has been a faculty member at the Biomedical Engineering Institute, Xi'an Jiaotong University, since 1986, where he teaches electrical neurophysiology and biomedical signal processing. His research interests include functional neuromuscular stimulation, nerve modeling, and biomedical signal processing.

Dr. Tai was named the excellent graduate student of Xi'an Jiaotong University in 1986.